

ARTICLES

Search for $B \rightarrow \mu \bar{\nu}_\mu \gamma$ and $B \rightarrow e \bar{\nu}_e \gamma$

T. E. Browder,¹ F. Li,¹ Y. Li,¹ J. L. Rodriguez,¹ T. Bergfeld,² B. I. Eisenstein,² J. Ernst,² G. E. Gladding,² G. D. Gollin,² E. Johnson,² I. Karliner,² M. Palmer,² M. Selen,² J. J. Thaler,² K. W. Edwards,³ A. Bellerive,⁴ D. I. Britton,⁴ R. Janicek,⁴ D. B. MacFarlane,⁴ K. W. McLean,⁴ P. M. Patel,⁴ A. J. Sadoff,⁵ R. Ammar,⁶ P. Baringer,⁶ A. Bean,⁶ D. Besson,⁶ D. Copping,⁶ C. Darling,⁶ R. Davis,⁶ N. Hancock,⁶ S. Kotov,⁶ I. Kravchenko,⁶ N. Kwak,⁶ S. Anderson,⁷ Y. Kubota,⁷ M. Lattery,⁷ J. J. O'Neill,⁷ S. Patton,⁷ R. Poling,⁷ T. Riehle,⁷ A. Smith,⁷ V. Savinov,⁷ M. S. Alam,⁸ S. B. Athar,⁸ Z. Ling,⁸ A. H. Mahmood,⁸ H. Severini,⁸ S. Timm,⁸ F. Wappler,⁸ A. Anastassov,⁹ S. Blinov,^{9,*} J. E. Duboscq,⁹ R. Fulton,⁹ D. Fujino,⁹ K. K. Gan,⁹ T. Hart,⁹ K. Honscheid,⁹ H. Kagan,⁹ R. Kass,⁹ J. Lee,⁹ M. Sung,⁹ A. Undrus,^{9,*} R. Wanke,⁹ A. Wolf,⁹ M. M. Zoeller,⁹ B. Nemati,¹⁰ S. J. Richichi,¹⁰ W. R. Ross,¹⁰ P. Skubic,¹⁰ M. Wood,¹⁰ M. Bishai,¹¹ J. Fast,¹¹ E. Gerndt,¹¹ J. W. Hinson,¹¹ D. H. Miller,¹¹ E. I. Shibata,¹¹ I. P. J. Shipsey,¹¹ M. Yurko,¹¹ L. Gibbons,¹² S. D. Johnson,¹² Y. Kwon,¹² S. Roberts,¹² E. H. Thorndike,¹² C. P. Jessop,¹³ K. Lingel,¹³ H. Marsiske,¹³ M. L. Perl,¹³ S. F. Schaffner,¹³ D. Ugolini,¹³ R. Wang,¹³ X. Zhou,¹³ T. E. Coan,¹⁴ V. Fadeyev,¹⁴ I. Korolkov,¹⁴ Y. Maravin,¹⁴ I. Narsky,¹⁴ V. Shelkov,¹⁴ R. Stroynowski,¹⁴ J. Staeck,¹⁴ I. Volobouev,¹⁴ J. Ye,¹⁴ M. Artuso,¹⁵ A. Efimov,¹⁵ M. Gao,¹⁵ M. Goldberg,¹⁵ R. Greene,¹⁵ F. Frasconi,¹⁵ D. He,¹⁵ S. Kopp,¹⁵ G. C. Moneti,¹⁵ R. Mountain,¹⁵ Y. Mukhin,¹⁵ S. Schuh,¹⁵ T. Skwarnicki,¹⁵ S. Stone,¹⁵ X. Xing,¹⁵ J. Bartelt,¹⁶ S. E. Csorna,¹⁶ V. Jain,¹⁶ S. Marka,¹⁶ A. Freyberger,¹⁷ R. Godang,¹⁷ D. Gibaut,¹⁷ K. Kinoshita,¹⁷ I. C. Lai,¹⁷ P. Pomianowski,¹⁷ S. Schrenk,¹⁷ G. Bonvicini,¹⁸ D. Cinabro,¹⁸ L. P. Perera,¹⁸ B. Barish,¹⁹ M. Chadha,¹⁹ S. Chan,¹⁹ G. Eigen,¹⁹ J. S. Miller,¹⁹ C. O'Grady,¹⁹ M. Schmittler,¹⁹ J. Urheim,¹⁹ A. J. Weinstein,¹⁹ F. Würthwein,¹⁹ D. M. Asner,²⁰ D. W. Bliss,²⁰ W. S. Brower,²⁰ G. Masek,²⁰ H. P. Paar,²⁰ J. Gronberg,²¹ C. M. Korte,²¹ D. J. Lange,²¹ R. Kutschke,²¹ S. Menary,²¹ R. J. Morrison,²¹ S. Nakanishi,²¹ H. N. Nelson,²¹ T. K. Nelson,²¹ C. Qiao,²¹ J. D. Richman,²¹ D. Roberts,²¹ A. Ryd,²¹ H. Tajima,²¹ M. S. Witherell,²¹ R. Balest,²² B. H. Behrens,²² K. Cho,²² W. T. Ford,²² H. Park,²² P. Rankin,²² J. Roy,²² J. G. Smith,²² J. P. Alexander,²³ C. Bebek,²³ B. E. Berger,²³ K. Berkelman,²³ K. Bloom,²³ D. G. Cassel,²³ H. A. Cho,²³ D. M. Coffman,²³ D. S. Crowcroft,²³ M. Dickson,²³ P. S. Drell,²³ R. Ehrlich,²³ R. Elia,²³ A. D. Foland,²³ P. Gaidarev,²³ B. Gittelman,²³ S. W. Gray,²³ D. L. Hartill,²³ B. K. Heltsley,²³ P. I. Hopman,²³ S. L. Jones,²³ J. Kandaswamy,²³ N. Katayama,²³ P. C. Kim,²³ D. L. Kreinick,²³ T. Lee,²³ Y. Liu,²³ G. S. Ludwig,²³ J. Masui,²³ J. Mevissen,²³ N. B. Mistry,²³ C. R. Ng,²³ E. Nordberg,²³ M. Ogg,^{23,†} J. R. Patterson,²³ D. Peterson,²³ D. Riley,²³ A. Soffer,²³ C. Ward,²³ P. Avery,²⁴ M. Athanas,²⁴ C. D. Jones,²⁴ M. Lohner,²⁴ C. Prescott,²⁴ S. Yang,²⁴ J. Yelton,²⁴ J. Zheng,²⁴ G. Brandenburg,²⁵ R. A. Briere,²⁵ D. Y.-J. Kim,²⁵ T. Liu,²⁵ M. Saulnier,²⁵ R. Wilson,²⁵ and H. Yamamoto²⁵

(CLEO Collaboration)

¹University of Hawaii at Manoa, Honolulu, Hawaii 96822²University of Illinois, Champaign-Urbana, Illinois 61801³Carleton University, Ottawa, Ontario, Canada K1S 5B6
and the Institute of Particle Physics, Canada⁴McGill University, Montréal, Québec, Canada H3A 2T8
and the Institute of Particle Physics, Canada⁵Ithaca College, Ithaca, New York 14850⁶University of Kansas, Lawrence, Kansas 66045⁷University of Minnesota, Minneapolis, Minnesota 55455⁸State University of New York at Albany, Albany, New York 1222⁹Ohio State University, Columbus, Ohio 43210¹⁰University of Oklahoma, Norman, Oklahoma 73019¹¹Purdue University, West Lafayette, Indiana 47907¹²University of Rochester, Rochester, New York 14627¹³Stanford Linear Accelerator Center, Stanford University, Stanford, California 94309¹⁴Southern Methodist University, Dallas, Texas 75275¹⁵Syracuse University, Syracuse, New York 13244

*Permanent address: BINP, RU-630090 Novosibirsk, Russia.

†Permanent address: University of Texas, Austin, TX 78712.

¹⁶Vanderbilt University, Nashville, Tennessee 37235

¹⁷Virginia Polytechnic Institute and State University, Blacksburg, Virginia 24061

¹⁸Wayne State University, Detroit, Michigan 48202

¹⁹California Institute of Technology, Pasadena, California 91125

²⁰University of California, San Diego, La Jolla, California 92093

²¹University of California, Santa Barbara, California 93106

²²University of Colorado, Boulder, Colorado 80309-0390

²³Cornell University, Ithaca, New York 14853

²⁴University of Florida, Gainesville, Florida 32611

²⁵Harvard University, Cambridge, Massachusetts 02138

(Received 12 November 1996)

We have searched for the decays $B \rightarrow \mu \bar{\nu}_\mu \gamma$ and $B \rightarrow e \bar{\nu}_e \gamma$ in a sample of 2.7×10^6 charged B decays collected with the CLEO II detector. In the muon channel, we observe no candidates in the signal region and set an upper limit on the branching fraction of $\mathcal{B}(B \rightarrow \mu \bar{\nu}_\mu \gamma) < 5.2 \times 10^{-5}$ at the 90% confidence level. In the electron channel, we observe five candidates in the signal region and set an upper limit on the branching fraction of $\mathcal{B}(B \rightarrow e \bar{\nu}_e \gamma) < 2.0 \times 10^{-4}$ at the 90% confidence level. [S0556-2821(97)05313-7]

PACS number(s): 13.20.He, 13.40.Hq, 14.40.Nd

In the standard model, measurements of V_{ub} , the Cabibbo-Kobayashi-Maskawa (CKM) mixing angle, and x_d , the $B^0 \bar{B}^0$ mixing parameter, can be used to place constraints on ρ and η , the unknown CKM constants of the Wolfenstein parametrization [1,2]. However, the constraint from $B^0 \bar{B}^0$ mixing depends on the unmeasured quantity f_B , the B decay constant. Theoretical estimates of f_B vary from 190 MeV by QCD sum rules [3] to around 370 MeV by lattice QCD calculations in the static quark limit [4]. The only direct experimental means to access f_B is through an observation of the purely leptonic decay $B \rightarrow l \nu_l$. (Throughout this paper, decays of the type $B \rightarrow l \bar{\nu}_l X$ refer to both $B^- \rightarrow l^- \bar{\nu}_l X$ and $B^+ \rightarrow l^+ \nu_l X$.) Both CLEO [5] and ALEPH [6] have published upper limits for $B \rightarrow l \bar{\nu}_l$. However, these limits are at least an order of magnitude larger than decay rates predicted by the standard model, which are helicity suppressed. In this paper, we describe first results from an alternative method of determining f_B through leptonic decays involving hard photon emission.

According to the model of Burdman, Goldman, and Wyler (BGW) [7], the decay rate for $B \rightarrow l \bar{\nu}_l \gamma$ is dominated by structure-dependent (SD) photon emission. In the SD process, a photon is produced in the transition of a spin-0 B meson to a spin-1 off-shell vector or axial-vector B meson. Because the heavy intermediate state has spin-one, helicity suppression does not occur. Hence, the SD process is suppressed only by the photon coupling. The decay rate depends on the mass difference between the initial- and intermediate-state B meson, the strength of the photon coupling to the heavy- and light-quark pieces of the electromagnetic current, and the decay constant of the intermediate-state B meson. These constants are expected to differ for transitions involving an intermediate-state vector (B^*) and axial-vector (B') mesons. While the $B^* - B$ and $B' - B$ mass differences are measured directly [8,9] the photon coupling constants (μ^* , μ'_j) are estimated from a combination of charm system measurements and theory [10]. Therefore, to a first approximation, the only uncertain parameters are the decay constants f_B^* and f_{B_j}' .

Since heavy quark symmetry (HQS) [11] cannot relate the decay constants of heavy mesons belonging to different spin

doublets, it is useful to define the relative strength of the axial-vector and vector processes as:

$$\gamma_j \equiv \frac{\mu'_j f_{B_j}'}{\mu^* f_B^*}. \quad (1)$$

If γ_j is small, an observation of $B \rightarrow l \bar{\nu}_l \gamma$ would provide a measurement of f_B^* . Knowledge of f_B^* , together with the HQS relation $f_B^* = m_B f_B$ [12], would then provide an alternative (albeit model-dependent) means to determine f_B . We might expect γ_j to be small because nonrelativistic models predict $f_{B_j}' = 0$. However, relativistic effects could result in values up to $\gamma_j = 1$ [13]. Currently, there are no experimental data based on which one can estimate the magnitude of γ_j . In this paper, we assume $\gamma_j = 0$.

Because $B \rightarrow l \bar{\nu}_l \gamma$ is not helicity suppressed, its decay rate is expected to be comparable to or larger than that for $B \rightarrow l \bar{\nu}_l$ decays. In addition, to first order in $(m_l/m_B)^2$, the decay rate is independent of the lepton species. The expected range for the $B \rightarrow l \bar{\nu}_l \gamma$ branching fraction is [7]

$$1.0 \times 10^{-6} < \mathcal{B}(B \rightarrow l \bar{\nu}_l \gamma) < 4.0 \times 10^{-6}, \quad (2)$$

where we have used $\tau_B = 1.6$ ps, $f_B^* = 1.0$ GeV², and $V_{ub} = 0.003$ as reasonable estimates for these parameters [14–16]. If we take $\mathcal{B}(B \rightarrow l \bar{\nu}_l \gamma) = 4.0 \times 10^{-6}$, then $\mathcal{B}(B \rightarrow \mu \bar{\nu}_\mu \gamma) \approx 16 \times \mathcal{B}(B \rightarrow \mu \bar{\nu}_\mu)$. This paper will focus on a search for $B \rightarrow e \bar{\nu}_e \gamma$ and $B \rightarrow \mu \bar{\nu}_\mu \gamma$.

We search for events in which there is an energetic lepton-photon pair and the remaining particles are consistent with the decay of a second B . One lepton-photon candidate per event is selected using the most energetic lepton and most energetic photon in the event. According to the BGW model, the lepton energy spectrum for $B \rightarrow l \bar{\nu}_l \gamma$ is slightly more peaked at high energies than what would be expected from phase space alone and has a mean value of 2.0 GeV. The photon energy spectrum has an inverted-parabolic shape with a mean value 1.3 GeV. The energy spectra of the lepton and photon as predicted by the BGW model are shown in Fig. 1. The constraints involving particles from the second

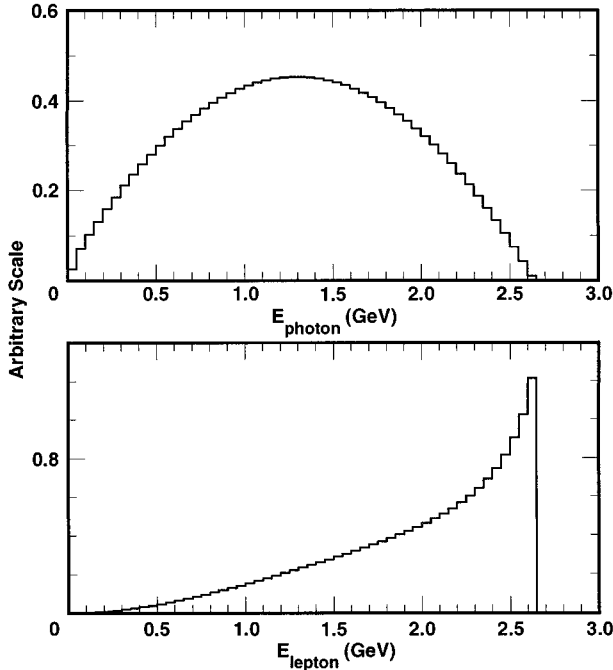


FIG. 1. The lepton and photon spectra of $B \rightarrow l \nu \gamma$ decays in the B rest frame (BGW model).

B are enforced by requiring that the invariant mass and energy of all detected particles except the lepton-photon pair be consistent with the B mass and beam energy, respectively. We also require that the missing energy and missing momentum of the signal candidate be consistent with an undetected neutrino.

The data used in this search were collected with the CLEO II detector [17] operating at the Cornell Electron Storage Ring (CESR). The data consist of approximately 2.7×10^6 $Y(4S) \rightarrow B\bar{B}$ events collected along with 9.6×10^6 continuum events at the $Y(4S)$ resonance at $\sqrt{s} = 10.58$ GeV (the “on-resonance” sample). We also use a sample of 5.0×10^6 continuum events collected below resonance at $\sqrt{s} = 10.52$ GeV for background subtraction (the “off-resonance” sample). The on- and off-resonance samples correspond to integrated luminosities of 2.5 fb^{-1} and 1.3 fb^{-1} , respectively.

The features of the CLEO II detector relevant to this analysis are described here. The trajectories of charged particles are reconstructed using a system of three concentric wire chambers covering 95% of $4\pi sr$ in an axial magnetic field of 1.5 T. A CsI electromagnetic calorimeter covering 98% of $4\pi sr$ detects photons with energies above 30 MeV. Photon candidates are identified by showers in the calorimeter that are not matched to tracks reconstructed in the tracking chamber. Electrons above 1.8 GeV are identified using the momentum energy balance of tracks matched to showers in the calorimeter and the specific ionization (dE/dx) of tracks in the drift chamber. Muons are required to penetrate at least seven nuclear interaction lengths. This places a lower limit of approximately 2.0 GeV/ c on the muon momentum. Other charged particles are identified through their specific ionization in the main drift chamber. All charged tracks are assigned the pion mass unless they are

identified as leptons or their dE/dx is inconsistent with the pion mass hypothesis ($>2\sigma$) and consistent with either the kaon or proton mass hypothesis ($<2\sigma$).

We select hadronic events by requiring that there be at least four charged tracks and significant visible energy. Other continuum backgrounds (including two-photon events) are suppressed by requiring $|\cos\theta_{\text{miss}}| < 0.95$, where θ_{miss} is the angle between the missing momentum and the beam line, and also by requiring that the net measured electric charge of the event $\sum Q_i$ be no more than 2. These requirements also reduce the number of events containing particles that are lost down the beam pipe. To further suppress continuum decays, we select events that are spherical in shape by requiring that the ratio of the second and zeroth Fox-Wolfram moments [18] (R_2) be less than 0.25.

To identify signal candidates we select one lepton-photon candidate per event using the most energetic lepton and most energetic photon in the event. We then require that the energy E_2 and the invariant mass $M_2 \equiv \sqrt{E_{\text{beam}}^2 - |P_2|^2}$ of all particles in the event except the lepton-photon pair be consistent with coming from a single B decay. In particular, we require $4.8 \text{ GeV} < E_2 < 5.5 \text{ GeV}$ and $M_2 > 5.27 \text{ GeV}$. These requirements suppress events with missing charged tracks, additional neutrinos, and undetected or partially detected neutral hadrons. Finally, we reconstruct the energy and momentum of the undetected neutrino using the four-momentum of the lepton, photon, and the second B . We define the neutrino energy and momentum as $E_\nu = E_{\text{beam}} - E_l - E_\gamma$ and $P_\nu = |\vec{P}_l + \vec{P}_\gamma + 0.320\hat{p}_2|$, respectively, where \hat{p}_2 is the unit-vector momentum of the second B . The correction term $0.320\hat{p}_2$ is needed to account for the momentum of the parent B (expressed in units of GeV/ c). To select signal events, we require $|E_\nu - P_\nu| < 200 \text{ MeV}$.

Backgrounds to $B \rightarrow l \bar{\nu}_l \gamma$ from generic $b \rightarrow cl \bar{\nu}_l$ and $b \rightarrow ul \bar{\nu}_l$ decays frequently occur when the primary lepton is combined with a photon from a π^0 decay. To suppress these backgrounds, we calculate the invariant mass $M_{\gamma\gamma}$ of the candidate photon (the most energetic photon) with respect to all other showers in the event. If any of the $M_{\gamma\gamma}$ combinations are consistent with the π^0 mass ($110 \text{ MeV} < M_{\gamma\gamma} < 160 \text{ MeV}$), the event is discarded. To further suppress $b \rightarrow cl \bar{\nu}_l$ decays, we require that the cosine of the lepton-photon opening angle, $\cos\theta_{l,\gamma}$, be less than zero. This requirement is efficient for signal decays, where the lepton and photon are often produced back to back. However, for $b \rightarrow cl \bar{\nu}_l$ events, the decay kinematics and the neutrino mass constraint together favor a small lepton-photon opening angle.

The probability that a $B \rightarrow \mu \bar{\nu}_\mu \gamma$ decay satisfies all selection criteria and lies in the signal region is $(1.93 \pm 0.04)\%$. The corresponding probability for a $B \rightarrow e \bar{\nu}_e \gamma$ decay is $(2.06 \pm 0.14)\%$. These probabilities are determined using a Monte Carlo simulation with the corrections described below. The error on each probability is statistical only.

For the $B \rightarrow \mu \bar{\nu}_\mu \gamma$ analysis, the mean number of on (off)-resonance candidates expected from background Monte Carlo simulation to fall into the $E_\nu - P_\nu$ sideband, defined by $200 \text{ MeV} < E_\nu - P_\nu < 2 \text{ GeV}$, is 41.3 ± 3.8 (1.0 ± 0.6). Of this yield, 93% comes from $b \rightarrow c \mu \bar{\nu}_\mu$ decays where the primary muon is the lepton candidate. A much smaller background

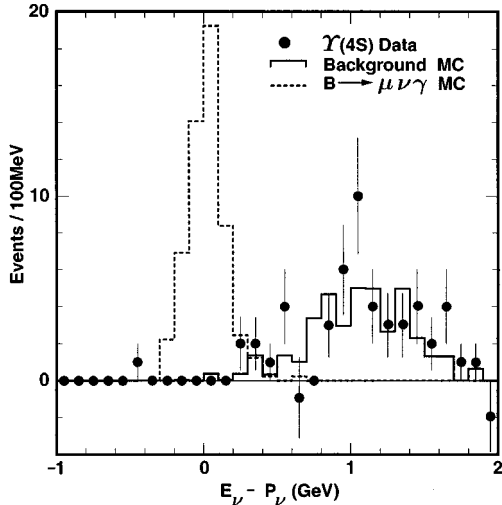


FIG. 2. The $E_\nu - P_\nu$ distribution for $B \rightarrow \mu \bar{\nu}_\mu \gamma$ event candidates. The signal region is defined by $|E_\nu - P_\nu| < 200$ MeV. An overlay is shown of on- $\Upsilon(4S)$ resonance minus scaled off- $\Upsilon(4S)$ resonance data (filled circles), the Monte Carlo background prediction (solid line), and the Monte Carlo signal prediction for a branching fraction $\beta(B \rightarrow \mu \bar{\nu}_\mu \gamma) = 1.1 \times 10^{-3}$ (dotted line).

comes from $q\bar{q}$ events (6%) and $b \rightarrow u \mu \bar{\nu}_\mu$ decays (1%). The normalization of the background is determined using the known values for the $B\bar{B}$ and continuum $q\bar{q}$ cross sections. The mean number of background candidates in the signal region is predicted to be 0.5 ± 1.1 . The number of on (off)-resonance candidates in the data that fall into the $E_\nu - P_\nu$ sideband is 51.0 ± 7.1 (2.0 ± 1.4). A comparison of the Monte Carlo simulation and data $E_\nu - P_\nu$ distributions is shown in Fig. 2; their agreement helps confirm our understanding of the normalization and composition of the background. No candidates in either the on- or off-resonance sample fall into the signal region. We obtain an upper limit on the signal yield based on zero candidates.

For the $B \rightarrow e \bar{\nu}_e \gamma$ analysis, the mean number of on (off)-resonance candidates expected from background Monte Carlo simulation to fall into the $E_\nu - P_\nu$ sideband is 79.9 ± 5.2 (1.3 ± 0.6). Of this yield, 97% comes from $b \rightarrow c e \bar{\nu}_e$ decays where the primary electron is the lepton candidate. The remainder of the background comes from $q\bar{q}$ events (2.4%) and $b \rightarrow u e \bar{\nu}_e$ decays (0.6%). The total number of background candidates in the signal region is predicted to be 0.1 ± 0.7 . To obtain an alternative estimate of this yield, we assume a uniform background distribution in the E_2 and M_2 sidebands, and determine the number of candidates in the signal region by extrapolation. Using this method, we obtain an estimate of 1.6 ± 0.1 candidates. This yield is reduced to 1.3 ± 0.1 if we take into account the typical falloff in the M_2 background distribution above 5.285 GeV [19]. The number of on (off)-resonance candidates in the data that fall into the $E_\nu - P_\nu$ sideband is 88.0 ± 9.4 (1.0 ± 1.0). While the data and the Monte Carlo background agree well in the $E_\nu - P_\nu$ sideband, they do not agree in the signal region, where we observe five on-resonance candidates and zero off-resonance candidates (see Fig. 3).

Each of the five candidate signal events was individually examined. These events are inconsistent with a two-photon

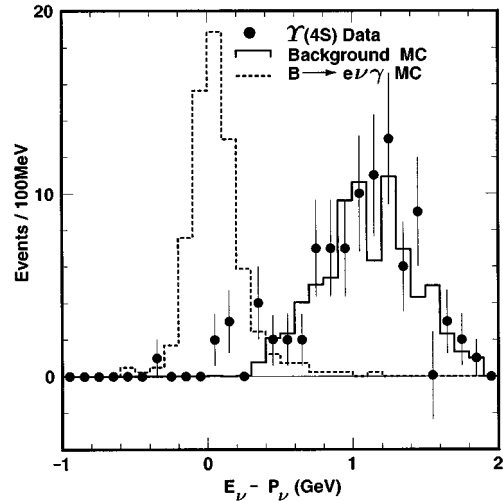


FIG. 3. The $E_\nu - P_\nu$ distribution for $B \rightarrow e \bar{\nu}_e \gamma$ event candidates. The signal region is defined by $|E_\nu - P_\nu| < 200$ MeV. An overlay is shown of on- $\Upsilon(4S)$ resonance minus scaled off- $\Upsilon(4S)$ resonance data (filled circles), the Monte Carlo background prediction (solid line), and the Monte Carlo signal prediction for a branching fraction $\beta(B \rightarrow e \bar{\nu}_e \gamma) = 1.3 \times 10^{-3}$ (dotted line).

interaction based on the correlation between the lepton-candidate direction and the beam direction [20]. The candidate events are also not consistent with being beam-related background or events containing lepton candidates from photon conversions and $J/\psi \rightarrow e^+ e^-$ decays. We also consider whether the candidate events could be a product of an upward statistical fluctuation of known backgrounds. If we assume a predicted background of 1.3 candidates, the probability of observing five or more candidates is 1%. In summary, we do not find any specific background processes which would give rise to these five candidate events nor do we believe it possible that fluctuations of known background contributions can explain these events. However, since most models, both the standard model and models beyond the

TABLE I. Signal efficiency for the $B \rightarrow l \nu \gamma$ analysis.

| Cut | $B \rightarrow \mu \nu \gamma$ | $B \rightarrow e \nu \gamma$ |
|------------------------------------------------------------------------------|--------------------------------|------------------------------|
| Lepton detection and identification and $P_l > 1.8$ GeV | 0.40 | 0.46 |
| Photon selection | 0.84 | 0.84 |
| $ \cos \theta_{\text{miss}} < 0.95$ | 0.97 | 0.96 |
| Hadronic event selection | 0.96 | 0.96 |
| $\Sigma Q_i \leq 2$ | 0.99 | 0.99 |
| $110 \text{ MeV} > M_{\gamma\gamma}$ or $M_{\gamma\gamma} > 160 \text{ MeV}$ | 0.69 | 0.66 |
| $R_2 < 0.25$ | 0.62 | 0.64 |
| $4.8 \text{ GeV} < E_{B_2} < 5.5 \text{ GeV}$ | 0.31 | 0.31 |
| $\cos \theta_{l,\gamma} < 0.0$ | 0.83 | 0.82 |
| $M_{B_2} > 5.23 \text{ GeV}$ | 0.62 | 0.60 |
| $-0.2 \text{ GeV} < E_\nu - P_\nu < 0.2 \text{ GeV}$ | 0.87 | 0.79 |
| Total efficiency | 0.019 | 0.021 |

TABLE II. Efficiency corrections and systematic uncertainties on the signal detection efficiency. The corrections are percentage changes to the efficiency.

| Requirement | Efficiency correction | | Systematic uncertainty |
|------------------------------------------------|-----------------------|-------|------------------------|
| | μ | e | |
| Lepton selection | 0 | 0 | $\pm 5.0\%$ |
| Photon selection | +0.7% | +0.7% | $\pm 0.4\%$ |
| $R_2 \cup E_2 \cup M_2$ | -8.0% | -8.0% | $\pm 13.4\%$ |
| π^0 veto | +0.7% | +0.7% | $\pm 3.7\%$ |
| $P_e > 1.8$ GeV | | -2.5% | $\pm 0.01\%$ |
| $B \rightarrow \mu \bar{\nu}_\mu \gamma$ total | -6.7% | | $\pm 14.8\%$ |
| $B \rightarrow e \bar{\nu}_e \gamma$ total | | -9.0% | $\pm 14.8\%$ |

standard model, would predict that the branching fraction for the electronic and the muonic modes are equal, the absence of muonic signal makes it inappropriate to regard these five electronic events as positive evidence for the radiative leptonic decay of the B . Therefore, since we were not able to identify the source of background giving rise to these five events, we must assume that they are a possible signal when we calculate an upper limit.

The contributions to the signal detection efficiency by various requirements we impose are listed in Table I. The efficiencies have been checked with independent data samples and corrected where necessary. In particular, the efficiencies for the E_2 , M_2 , and R_2 requirements are checked using the remaining particles in events in which one of the two B decays has been reconstructed as $B \rightarrow D^* l \bar{\nu}_l$ [21]. A systematic correction on the combined efficiency for the E_2 , M_2 , and R_2 is estimated to be 0.920 ± 0.134 by comparing $B \rightarrow D^* l \bar{\nu}_l$ events in Monte Carlo simulation and data. The uncertainty on this correction is dominated by the statistics of the study. The efficiency for the π^0 veto is checked by calculating $M_{\gamma\gamma}$ of a signal photon with respect to all other photons in generic BB Monte Carlo simulation and data events. The resulting correction factor is 1.007 ± 0.037 , where the error is statistical. Other smaller systematic effects related to lepton selection, photon selection, and the electroweak correction to the electron momentum spectrum have also been studied [22]. A summary of these systematic studies is given in Table II.

Uncertainties on the signal detection efficiency also arise from an incomplete knowledge of γ_j in the BGW model. In particular, large values of γ_j imply a greater admixture of

axial-vector meson decays which results in a harder photon energy spectrum and softer lepton spectrum. Since both high-energy leptons *and* photons are favored by the event selection criteria, larger values of γ_j simultaneously increase the photon selection efficiency and decrease the lepton selection efficiency. To study the net systematic effect on the signal detection efficiency, we use a signal Monte Carlo simulation with the opposite extreme value for the relative axial-vector strength $\gamma_j = 1$, and find that the signal detection efficiency increases by a factor of 1.039 ± 0.040 . Since we are measuring upper limits for $B \rightarrow \mu \bar{\nu}_\mu \gamma$ and $B \rightarrow e \bar{\nu}_e \gamma$, the choice $\gamma_j = 0$ in our BGW Monte Carlo simulation leads to a conservative estimate of the efficiency.

The total uncertainty on the signal detection efficiency is obtained by adding the systematic uncertainty ($\pm 14.8\%$) and statistical uncertainty ($\pm 1.9\%$ for $B \rightarrow \mu \bar{\nu}_\mu \gamma$ and $\pm 6.7\%$ for $B \rightarrow e \bar{\nu}_e \gamma$) in quadrature. In addition, there is an uncertainty of $\pm 1.8\%$ in the number of $B^+ B^-$ events in our data sample.

To calculate an upper limit on the number of signal candidates observed, we use Poisson statistics [23]. If we regard all on-resonance candidates that pass the event selection criteria as signal candidates, we obtain an upper limit on the signal yield for $B \rightarrow \mu \bar{\nu}_\mu \gamma$ and $B \rightarrow e \bar{\nu}_e \gamma$ of 2.3 and 9.3, respectively, at the 90% C.L. To calculate an upper limit on the branching fraction, the estimated signal detection efficiency is reduced by one standard deviation. This, combined with the total number of charged B decays in the data sample (2.7×10^6), gives

$$\mathcal{B}(B \rightarrow \mu \bar{\nu}_\mu \gamma) < 5.2 \times 10^{-5} \text{ (90\% C.L.)}, \quad (3)$$

$$\mathcal{B}(B \rightarrow e \bar{\nu}_e \gamma) < 2.0 \times 10^{-4} \text{ (90\% C.L.)}. \quad (4)$$

Using the upper limit on $\mathcal{B}(B \rightarrow \mu \bar{\nu}_\mu \gamma)$, the assumption $\gamma_j = 0$, and the allowed range of μ^* , we extract a range of limits on f_B^* . Given the lower (upper) limit for μ^* , we obtain $f_B^* < 7.25$ (3.62) GeV² at the 90% C.L. Using the HQS relation $f_B^* = m_B f_B$, we obtain $f_B < 1.37$ (0.69) GeV at the 90% C.L. For comparison, the constraint obtained from the upper limit on $B \rightarrow \tau \bar{\nu}_\tau$ [5] is $f_B < 1.23$ GeV at the 90% C.L.

We gratefully acknowledge the effort of the CESR staff in providing us with excellent luminosity and running conditions. This work was supported by the National Science Foundation, the U.S. Department of Energy, the Heisenberg Foundation, the Alexander von Humboldt Stiftung, the National Sciences and Engineering Research Council of Canada, and the A. P. Sloan Foundation.

[1] J. L. Rosner, in *B Decays*, edited by S. Stone (World Scientific, Singapore, 1992).
[2] L. Wolfenstein, Phys. Rev. Lett. **51**, 1945 (1983).
[3] M. Neubert, Phys. Rev. D **45**, 2451 (1992).
[4] C. R. Allton *et al.*, Nucl. Phys. **B349**, 598 (1991); C. Alexandrou *et al.*, Phys. Lett. B **256**, 60 (1991).
[5] CLEO Collaboration, M. Artuso *et al.*, Phys. Rev. Lett. **75**, 785 (1995).

[6] ALEPH Collaboration, D. Buskulic *et al.*, Phys. Lett. B **343**, 444 (1995).
[7] G. Burdman, T. Goldman, and D. Wyler, Phys. Rev. D **51**, 111 (1995).
[8] L. Montanet *et al.*, Phys. Rev. D **50**, 1639 (1994).
[9] DELPHI Collaboration, P. Abreu *et al.*, Phys. Lett. B **345**, 598 (1995).
[10] W. A. Bardeen and C. T. Hill, Phys. Rev. D **49**, 409 (1994).

- [11] N. Isgur and M. B. Wise, in *B Decays* [1].
- [12] N. Isgur and M. B. Wise, *Phys. Lett. B* **232**, 113 (1989).
- [13] G. Burdman (private communication); see also Ref. [7].
- [14] L. Montanet *et al.*, *Phys. Rev. D* **50**, 1609 (1994).
- [15] Calculated using the value $f_B = 190$ MeV and the HQS symmetry relation $f_B^* = m_B f_B$ [12].
- [16] J. Bartelt *et al.*, *Phys. Rev. Lett.* **71**, 4111 (1993).
- [17] CLEO Collaboration, Y. Kubota *et al.*, *Nucl. Instrum. Methods Phys. Res. A* **320**, 66 (1992).
- [18] G. Fox and S. Wolfram, *Phys. Rev. Lett.* **41**, 1581 (1978).
- [19] CLEO Collaboration, S. Henderson *et al.*, *Phys. Rev. D* **45**, 2212 (1992).
- [20] V. M. Budnev, I. F. Ginzburg, G. V. Meledin, and V. G. Serbo, *Phys. Rep.*, *Phys. Lett.* **15C**, 181 (1975).
- [21] This procedure is described in a similar context in [5].
- [22] M. Lattery, University of Minnesota dissertation, 1996.
- [23] L. Montanet *et al.*, *Phys. Rev. D* **50**, 1279 (1994).